

# INITIAL STUDIES OF LONGITUDINAL DYNAMICS ON UMER\*

J. R. Harris#, A. Valfells, B. Beaudoin, S. Bernal, A. Diep, I. Haber, Y. Huo, B. Quinn, M. Reiser, M. Walter, P.G. O'Shea, Institute for Research in Electronics and Applied Physics, University of Maryland, College Park, MD 20742, USA

## Abstract

The University of Maryland Electron Ring (UMER) is a small-scale experiment on space-charge dominated beams. The 100 ns, 10 keV electron beam fills up nearly one-half of the ring circumference. Here we review two models for the evolution of such beams, and present some initial results of measurements of longitudinal beam expansion for two initial line charge profiles.

## 1 INTRODUCTION

The University of Maryland Electron Ring (UMER) is a compact, low-energy transport system built to study the physics of space-charge dominated beams [1,2]. The beam is produced by a 10-keV electron gun with current adjustable from 550  $\mu$ A to 100 mA. This allows UMER to operate in both the transverse emittance dominated and transverse space-charge dominated regimes. UMER is designed with operating parameters that allow it to serve as a model system for beams of very high intensity in a strong focusing lattice such as those for spallation neutron sources or heavy ion inertial confinement fusion (HIF) drivers [3].

Longitudinal space-charge effects are an area of particular interest for both UMER and HIF. In UMER, the beam initially fills half the ring. Longitudinal space-charge forces will cause the beam to expand, ultimately filling the entire ring and making extraction impossible. For HIF, certain designs call for longitudinal compression of the beam to increase the beam density delivered to the target [4]. For both projects, an improved understanding of longitudinal effects is needed, including both free expansion and beam compression.

To this end, we are conducting a detailed study of longitudinal dynamics in UMER. Here we describe two models for the longitudinal behavior of space-charge dominated beams and report the initial results of longitudinal experiments on drifting beams.

## 2 THEORY

### 2.1 Longitudinal Envelope Equation

The most general description for the longitudinal behavior of beams is the longitudinal envelope equation (LEE) [5-10]. For a space-charge dominated beam with no focusing, the LEE becomes

$$\tilde{z}'' = \frac{K_L}{5\sqrt{5}\tilde{z}^2}. \quad (1)$$

\*This work supported by the U.S. Department of Energy  
#harrisjr@wam.umd.edu

Here  $\tilde{z}$  is the RMS length of the beam,  $K_L$  is the longitudinal generalized permeance, and the primes denote differentiation with respect to  $s$ , the distance traveled from the cathode. The generalized longitudinal permeance is given by

$$K_L = \frac{3}{2} \frac{gN}{\beta^2 \gamma^5} \frac{q^2}{4\pi\epsilon_0 mc^2} \quad (2)$$

where  $N$  is the total number of particles in the bunch,  $m$  is the mass of the electron,  $q$  is the charge of the electron, and  $\epsilon_0$ ,  $c$ ,  $\beta$ , and  $\gamma$  have their customary meanings. The geometry factor  $g$  is given approximately by

$$g \approx \alpha + 2 \ln\left(\frac{b}{a}\right) \quad (3)$$

where  $b$  is the radius of the beam pipe,  $a$  is the radius of the beam, and  $\alpha$  is a constant that is variously cited as 0 [11], 0.5 [12], 0.67 [5], or 1 [5].

The LEE is derived for a beam with a parabolic line charge density. However, in longitudinal theory the parabolic line charge density serves the same role that the K-V distribution serves in transverse theory. That is, the parabolic beam can be taken as an equivalent line charge density for a beam with the same number of particles, the same emittance, and the same RMS length [9]. Therefore the LEE may describe the evolution, in an RMS sense, of any beam.

### 2.2 One-Dimensional Cold Fluid Model

A second theory to describe the longitudinal evolution of beams is the one-dimensional cold fluid model (CFM). The CFM applies only to beams which are totally space-charge dominated. In the CFM, the longitudinal evolution of a beam is given by the one-dimensional continuity equation

$$\frac{\partial \lambda}{\partial t} + \frac{\partial}{\partial z} v\lambda = 0 \quad (4)$$

and the momentum equation [12]

$$\frac{\partial v}{\partial t} + v \frac{\partial v}{\partial z} \approx - \frac{qg}{4\pi\epsilon_0 m \gamma^5} \frac{\partial \lambda}{\partial z}. \quad (5)$$

Here  $\lambda$  is the local line charge density,  $z$  is the position in the rest frame of the beam,  $v$  is the local particle velocity in the rest frame of the beam, and  $t$  is time. Note that the momentum equation is the Euler equation for compressible fluid flow [13], with the pressure term

replaced by  $\frac{q}{m\gamma^3} E_{sz}$ , where

$$E_{sz} = \frac{-g}{4\pi\epsilon_0\gamma^2} \frac{\partial\lambda}{\partial z} \quad (6)$$

is the expression for the longitudinal space charge force in the beam in the limit of slowly varying  $\lambda$ , and  $m\gamma^3$  is the longitudinal effective mass [5]. In the special case of a beam with an initially rectangular line charge profile, these equations can be solved to describe the longitudinal erosion of the beam [14]. This erosion occurs through the propagation of a shock wave from each end of the beam towards the center at the speed of sound in the beam [4,10],

$$c_0 = \sqrt{\frac{qg\lambda_0}{4\pi\epsilon_0 m\gamma^5}}. \quad (7)$$

As the shock wave passes a particle, it is accelerated, eventually reaching its escape velocity  $2c_0$ . The resulting line charge and velocity distributions for the leading edge of the beam are

$$\lambda(z,t) = \left( \frac{2}{3} \pm \frac{1}{3} \frac{z-z_0}{tc_0} \right)^2 \lambda_0 \quad (8a)$$

and

$$v(z,t) = \frac{2}{3} \left( \frac{z-z_0}{t} \mp c_0 \right). \quad (8b)$$

Here  $\lambda_0$  is the initial line charge density of the rectangular pulse,  $z$  is the location in the beam with  $z=0$  at the beam center,  $z_0$  is the initial location of the front or rear edge of the beam, and  $t$  is the time measured from  $t=0$  when the beam is created. The upper sign is used when considering erosion of the flat top from its rear edge, and the lower sign is used when considering erosion of the flat top from its leading edge. Equations (8a) and (8b) are only valid so long as the forward-traveling shockwave and the rear-traveling shockwave have not met. Once they meet, the flat top has been eliminated and the beam is "all ends." After this time, the shock waves which caused the flat top to erode begin to overlap, and the resulting nonlinear equations cannot be solved exactly. An approximate solution is given in Ref. [4].

### 3 EXPERIMENTS

#### 3.1 General

UMER is still under construction at this time, so the initial longitudinal measurements were taken using the existing portions of the machine, including the straight injection section (~1.5 m long) and 180° of arc of the ring. The total length of the existing sections used for longitudinal measurements is 7.54 m from the cathode to the last current monitor. The beam pipe radius in UMER is 25.4 mm, while the average beam radius in the ring's quadrupole focusing channel is 5.3 mm for the 24-mA beam and 9.5 mm for the 85-mA beam.

Measurements of the beam line charge profile were made using one Bergoz fast current transformer (FCT) and one fast beam position monitor (BPM) in the injection section, nine additional fast BPMs placed every 64 cm around the existing portions of the ring, and a second Bergoz FCT 48 cm after the last BPM. (During the actual experiment, the BPM at 5.78 m downstream from the cathode was not available.) The BPMs used for these measurements are designed to act as fast current monitors as well as to detect beam centroid position, and have a measured resolution (10%-90% rise time) of 1.7 ns [15]. An improved energy analyzer is currently under development and will be included in UMER in the near future [16].

#### 3.2 Expansion of Rectangular Beam

The standard initial beam profile produced in UMER is a rectangular pulse with length of 100 ns and rise time of approximately 2 ns produced by thermionic emission from a dispenser cathode. As a test of the CFM, the rise time of the beam was measured for 85-mA and 24-mA beams as they traveled through the existing 7.54 m of beam line. The 20%-80% rise time was used to limit the effects of detector circuit ringing on the measurement. The measured rise times were then compared to those predicted using Eq. (8a) (Fig. 1).

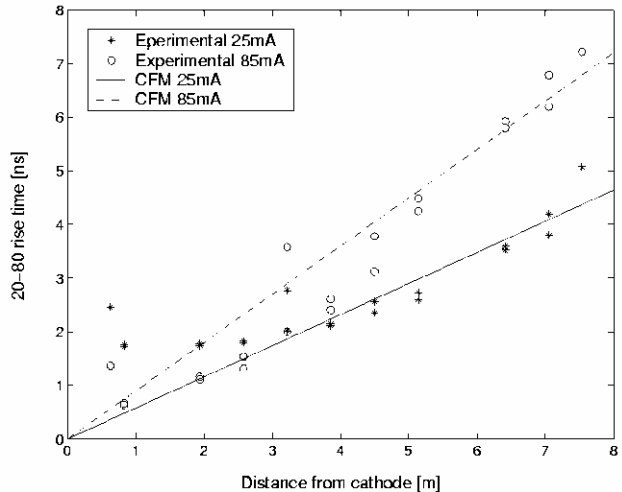


Figure 1: Increase in rise time of rectangular beam with distance from cathode for 85-mA and 24-mA beams.

For both current levels the increase of the rise time with distance from the cathode followed the linear trend predicted by Eq. (8a) after the beam had traveled through approximately half the existing transport line. For the 24-mA beam the observed rise time remained constant at 1.7 ns over the first 3 m of beam line. This may suggest that the expansion predicted by Eq. (8a), which assumes an initial perfect rectangular beam, is obscured by the ~2-ns initial beam rise time associated with the limitations of the gun and pulser. It is also possible that the beam rise time in this region is smaller than the BPMs or FCTs can detect. The 85-mA beam closely follows the expected linear trend after traveling 4.5 m from the cathode.

Before this point, the measured rise time is less than expected. The source of this discrepancy is unknown at this time.

A least-squares fit was made to the rise time data, assuming linear expansion beginning at the origin. Only data taken far from the cathode where the rate of increase was linear was included ( $s > 4.5$  m for 85 mA,  $s > 3.9$  m for 24 mA). These fits were compared with the expected rate of increase of the 20%-80% rise time based on Eq. (8a) in order to determine the value of the geometry factor  $g$ . The resulting values were  $g = 2.82$  for the 85-mA beam, and  $g = 4.25$  for the 24-mA beam. This gives  $\alpha = 0.85 \pm 0.25$  for the 85-mA beam and  $\alpha = 1.12 \pm 0.25$  for the 24-mA beam, and an average value of  $\langle \alpha \rangle = 0.985 \pm 0.25$ .

### 3.3 Expansion of Photoemission Beam

The UMER gun was designed for use with a dispenser cathode operating as a thermionic emission source. Recent work at Maryland has investigated the use of dispenser cathodes as photoemission sources [17]. As a byproduct of this research, UMER has been modified by the addition of an adjustable mirror inside the first diagnostics chamber, which allows the cathode to be illuminated from outside the beam pipe with laser light. The laser used on UMER is an Nd:YAG laser with some of its light shifted into the green with external nonlinear crystals. The laser pulse is 4.5 ns long, and Gaussian in profile. This allows us to produce short beams of Gaussian line charge profile in addition to longer rectangular pulses.

The longitudinal expansion of a 24 mA peak current beam was measured with the same FCTs and BPMs used to study the expansion of the rectangular beam. The averaged measurements at each location are plotted in Fig. 2.

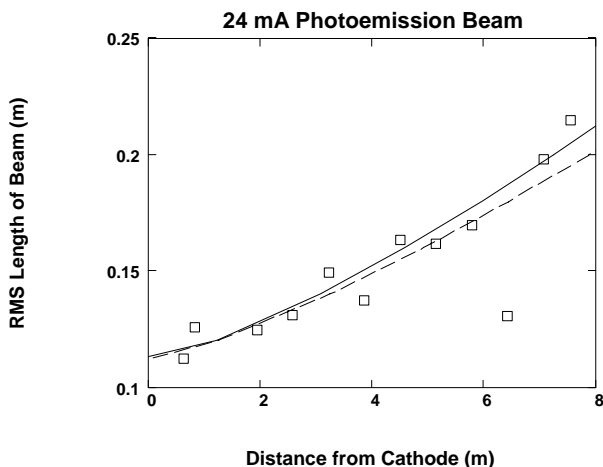


Figure 2: Increase in length of photoemission beam with 24 mA peak current. Curves are calculated from LEE using measured initial slope and length of beam. Solid curve is for  $\alpha = 1$  and dashed curve is for  $\alpha = 0$ .

Also shown in Fig. 2 are theoretical expansion curves calculated from the LEE assuming two values for  $\alpha$ . The initial beam length and initial rate of increase used to generate these curves were taken from experiment.

## 4 CONCLUSIONS

Initial experiments have commenced to study the longitudinal behavior of space-charge dominated beams in UMER. These experiments show expansion of beams with rectangular and Gaussian line charge profiles in the absence of focusing which is in agreement with the CFM and the LEE, respectively. Initial measurements of the constant  $\alpha$  suggest its value is approximately one.

## REFERENCES

- [1] Online: <http://www.ireap.umd.edu/umer/>
- [2] S. Bernal et al., "Beam Transport Experiments over a Single Turn at the University of Maryland Electron Ring (UMER)," these proceedings.
- [3] P.G. O'Shea et al., *Laser Part. Beams* (2002), 20, 599-602
- [4] D. D.-M. Ho, S.T. Brandon and E.P. Lee, "Longitudinal Beam Compression for Heavy-Ion Inertial Fusion," *Particle Accelerators*, 1991, Vol. 35, pp. 15-42.
- [5] M. Reiser, *Theory and Design of Charged Particle Beams*, Ch. 5.
- [6] L. Smith, et al., *ERDA Summer Study of Heavy Ions for Inertial Fusion: Final Report*, LBL-5543, Appendix 6-4, December 1976.
- [7] David Neuffer, "Extentions of the Longitudinal Envelope Equation," FERMILAB-TM-1993, April 1997.
- [8] Frank J. Sacherer, *IEEE Trans. Nucl. Sci.* **18**, p. 1105, 1971.
- [9] M. Reiser, Personal Communication, 19 Aug. 2001.
- [10] H.W. Liepmann and A. Roshko, *Elements of Gasdynamics*, Wiley, New York, 1967.
- [11] A. Faltens, E.P. Lee, and S.S. Rosenblum, *J. Appl. Phys.* **61** (12), 15 June 1987, p. 5219
- [12] G. Emanuel, *Analytical Fluid Dynamics*, CRC, Boca Raton, 2001.
- [13] Dunxiang Wang, *Experimental Studies of Longitudinal Dynamics of Space-Charge Dominated Electron Beams*. Doctoral Dissertation, University of Maryland, 1993.
- [14] I. Haber, et al., "Maryland Transport Experiment Comparison to Theory and Simulation." *Space Charge Dominated Beams and Applications of High Brightness Beams*. Ed. S.Y. Lee. AIP: Woodbury, N.Y. 1996
- [15] B. Quinn, et al., "Design and Testing of a Fast Beam Position Monitor," these proceedings.
- [16] Y. Cui, et al. "Experimental Study of Energy Spread in A Space-Charge Dominated Electron Beam," these proceedings.
- [17] D. Feldman, et al., "Development of Dispenser Cathodes for RF Photoinjectors," these proceedings.